Tanguy, M.; Baille, A.; Gonzalez-Real, M.M.; Lloyd, C.; Cappelaere, B.; Kergoat, L.; Cohard, J.-M.. 2012 A new parameterisation scheme of ground heat flux for land surface flux retrieval from remote sensing information. *Journal of Hydrology*, 454-455. 113-122. 10.1016/j.jhydrol.2012.06.002

.

A new parameterisation scheme of ground heat flux for land surface flux retrieval from remote sensing information

M. Tanguy [a,b], A. Baille [a] (*), M.M. González-Real [a], C. Lloyd [b], B. Cappelaere [c] , L. Kergoat [d], J-M. Cohard [e]

[a] Universidad Politécnica de Cartagena (UPCT), Paseo Alfonso XIII 48, 30203 Cartagena, Spain, maliko.tanguy@upct.es, mayla.gonreal@upct.es

[b] Centre for Ecology and Hydrology (CEH), Maclean Building, Benson Lane, Crowmarsh Gifford, Wallingford, Oxfordshire OX10 8BB, UK, crl@ceh.ac.uk

[c] Institut de Recherche pour le Développement (IRD), UMR HydroSciences Montpellier (CNRS/IRD/UM1/UM2) 911 Avenue Agropolis, 34394 Montpellier, France, bernard.cappelaere@um2.fr

[d] Géosciences Environnement Toulouse (GET), LMTG (CNRS/UPS/IRD), 14 avenue Édouard Belin, 31400 Toulouse, France, laurent.kergoat@get.obs-mip.fr

[e] Université Joseph Fourier (UJF), BP 53, 38041 Grenoble, cedex 9, France, jean-martial.cohard@ujf-grenoble.fr

(*) Corresponding author, Universidad Politécnica de Cartagena (UPCT), Paseo Alfonso XIII 48, 30203 Cartagena, Spain, baille.alain@upct.es, tel: +34-968325658, fax: +34-968 32 57 32

Abstract

The objective of the study was to assess the performance of a new parameterisation scheme of ground heat flux (G) for retrieving surface fluxes from remote sensing data (MODIS-Terra). Formulae that are based on empirical relationships relating G to net radiation, R_n ($G = \alpha R_n$, α being a function of a vegetation index, VI) are currently used, but presented drawbacks, especially in bare or sparse vegetation areas because of the poor adequacy of VI-based relationships to account for changes in soil moisture. In this study, we proposed to link α to the evaporative fraction, EF. In a first step, using a non-dimensional form of the surface energy balance, we demonstrated that α is functionally related to EF and to the ratio $\gamma = G/H$ (H = sensible heat flux). In a second step, we proposed an EF-based parameterisation of α, using ground fluxes data sets collected throughout the years 2005, 2006 and 2007 at four flux-tower sites in West African countries (Mali, Benin, Niger) that differ in surface conditions and Monsoon influence. The analysis indicated that the average site-specific values of α and EF were well described by a linear relationship of the type α = a EF + b, with a = -0.22 and b = 0.23. In a third stage, we investigated whether ET-retrieval from remote sensing information (MODIS-Terra) using the new parameterisation of α perform better than the classical formulation through VI-based relationships. We found that the retrieved values of H using the new parameterisation supplied the best agreement with the observed ground data and significant improvement with respect to estimates from α-VI relationships. Advantages and limitations of the proposed parameterisation scheme were discussed.

Key words: remote sensing, ground heat flux, sensible heat flux, evaporative fraction, vegetation index

1. Introduction

Knowledge and prediction of energy partitioning at the land surface is of primary importance in many issues related to the impact of land use on water resources and climate, desertification processes and land productivity, among others. In particular, evapotranspiration (ET) is an important component of the surface energy balance (SEB), whose knowledge is of high interest for the abovementioned issues. ET is a necessary input to global climate and hydrological models, and a direct output for applications to irrigation scheduling and agricultural water management. In fragile ecosystems such as the semi-arid regions of the African Sahelian belt, with scarce water resources and frequent drought events, adoption and fostering of suitable rainfed/irrigation practices are of paramount importance to maintain the balance between water demand and water resources. In these areas, characterising the spatial and temporal changes in ET constitutes valuable information to be used and integrated into early warning systems and water management tools (Zschau and Küppers, 2003; Boken, 2009; Hellegers et al., 2009).

Remote sensing (RS) data provided by optical sensors on board of Earth Observation (EO) satellites are currently used to estimate the spatial distribution of SEB components, by retrieving them from specific algorithms based on the closure of the energy balance equation:

$$R_n = \lambda E + H + G \quad (1)$$

where R_n is the net radiation, λE is the latent heat flux, H is the sensible heat flux and G is the soil heat flux.

Since the 1980s, there has been an increasing effort to develop methods for estimating ET from remote sensing data (among others: Norman et al., 1995; Bastiaanssen et al., 1998a, b; Carlson et al., 1995; Roerink et al., 2000; Nishida et al., 2003; Jiang et al., 2004; Courault et al., 2005). The potential of using thermal infrared observations from space has been widely explored and significant progress has been made, as underlined by recent papers reviewing the main methods to retrieve the evaporative fraction (*EF*) from remote sensing and summarizing the theoretical assumptions, advantages and limitations of each of them (Verstraeten et al., 2008; Li et al., 2009). Kalma et al. (2008) offer a comprehensive survey of published methods known to date, pointing out the main issues and challenges to address in the future. A critical point that has not been yet addressed in details in the assessment of the performance of the ET-retrieval methods is the uncertainty resulting from the parameterisation of the available energy term, $A = R_n - G$, and especially of the term G, which can reach high values in arid and semiarid countries. As the other fluxes, λE and H, are obtained from $\lambda E = A \times EF$ and $H = A \times (1 - EF)$, the importance to get a suitable parameterisation of both R_n and G is obvious. Concerning net radiation, there are several methods (e.g. Allen et al., 1998; Bisht et al., 2005; Batra, 2006) that can provide reliable estimations of area-average R_n using remote sensing information such as land surface temperature, albedo and atmospheric transmittance. The problem to get reliable estimates of G is much more complex, due to the combined effect of soil moisture and land surface properties on this flux.

Ground truth validation of RS algorithms is not straightforward because of the difficulty in obtaining reliable pixel-averaged values (e.g. 1 km^2) of the SEB components. If relatively accurate ground measurements of area-averaged λE and H can be obtained, generally by means of the eddy-covariance flux-towers (McCabe and Wood, 2006; Mu et al., 2007; Scott, 2010), the issue of getting reasonably-accurate measurements of area-averaged soil heat flux, G, is still to be resolved. The two main causes of the large errors in measuring are (i) the recognised lack of accuracy of the G measurement methods (see, among others, Oschner et al., 2006) and (ii) the sampling error in sparse vegetation covered areas. Even with a large network of sensors around the flux-tower, the footprint of G measurements remains very small compared to the footprint of the fluxes measured by eddy correlation (Schuttemeyer et al., 2006). The combination of the two types of errors results generally in rather imprecise ground data of G, and in large uncertainties when upscaling from point measurements to EC footprints or to large pixels. Prediction of G can be improved by means of analytical or numerical tools based on the resolution of the heat diffusion equation. The tools differ in their needs of local measurements of surface temperature, soil temperature profile, soil moisture, or air temperature (Wang and Bras, 1999; Verhoef, 2004, Murray and Verhoef, 2007a, b; Nunez et al., 2010. Wang and Bou-Zeid, 2012; Verhoef et al., 2012). These physically-based methods are universal, but highly demanding in input data and rather complex to handle.

The alternative to numerical methods is the empirical approach based on experimentally-derived relationships between G and one of the components of the surface energy balance equation. The simplest approach is to consider G as a constant fraction of R_n ($\alpha = G/R_n$). Typical recommended values for α range from 0.15 to 0.40

in the literature for different types of surface (Brutsaert, 1982; Choudhury, 1987; Humes et al., 1994; Kustas and Goodrich, 1994). Although this approach has been widely applied (Deardorff, 1978; Norman et al., 1995, 2000; Mecikalski et al., 1999; Crawford et al, 2000) many studies have shown that α is not constant in space or in time and is highly dependent on soil moisture, soil texture and vegetation cover (Clothier et al., 1986; Kustas et al., 1993). Therefore another commonly used approach is the estimation of α as a function of R_n and a vegetation index (VI), generally NDVI (Kustas and Daughtry, 1990; Moran et al., 1994; Bastiaanssen et al., 1998a; Jacobsen and Hansen, 1999; Friedl, 2002). In the last years, the parameterisation proposed by Su (2002) using the cover fraction (f_c) as predictive variable was often adopted (e.g., Tang, 2010), appearing as a standard empirical method for retrieving G. Although such a formulation allows accounting for the effect of vegetation cover on G, it presents drawbacks in bare or sparse vegetation areas due to the low responsiveness of VIs to changes in soil moisture conditions and to the weak correlation between instantaneous values of G and weekly or biweekly estimates of vegetation indices.

An alternative to parameterise G is to consider that G is more closely linked to the sensible heat flux, H, than to R_n. This hypothesis was used since the 70s to estimate G in atmospheric circulation models. Bhumralkar (1975) tested the relationship $G = \gamma H$ (with γ = constant throughout the day = 0.30) and compared its performance with other parameterization schemes. The experimental study of Berkowicz and Prahm (1982) concluded that G can be considered proportional to H in three contrasted sites, while Cellier et al. (1996) parameterized the ratio G/H as a function of daily mean wind speed. However, Liebethal and Foken (2007) evaluated six parameterisation approaches for G, concluding that H-based relationships do not supply the best performances among the tested approaches.

In this study, we hypothesised that more realistic estimates of G could be obtained by directly linking the parameter α to the evaporative fraction, *EF*, the latter being more responsive than VIs to soil moisture in sparse vegetated areas. We first demonstrated that the parameters α and γ are linked to the evaporative fraction by a functional relationship, and that both could be expressed as a function of EF, therefore providing a theoretical basis for our basic assumption. In a second step, we proposed an EF-based parameterisation of α, using ground flux data sets obtained at four flux-tower sites in West African countries (Mali, Benin, Niger) that differ in surface conditions and Monsoon influence. Finally, we investigated whether the ET-retrieval method using the new parameterisation of α could perform better than the classical formulation through VI-based relationships.

2. Materials and Methods

2.1. Sites description

The data used for the validation in this study were provided by sites managed by AMMA (African Monsoon Multidisciplinary Analysis) partners within the AMMA-Catch observation system (Lebel et al., 2009). Information on AMMA project can be found at http://amma-international.org/. One of the main objectives of AMMA was to improve the knowledge and understanding of the West African monsoon and its variability with an emphasis on daily-to-interannual timescale. Figure 1 shows the location of the sites used in this study, which have contributed ground truth to previous analyses of remote sensing data (Kergoat et al., 2011). The ground data used in this study included mainly net radiation, sensible heat flux, soil moisture at two depths and rainfall.

2.1.1. Eguerit and Kelma sites (Mali)

Mean annual rainfall over these two sites is around 370 mm, occurring from June to September with no rain at all from October to April (Frappart et al., 2009). The landscape is dominated by grasslands growing on sandy dunes. Bare soil is also widely present in the area, either with rocks topped with gravels or loamy shallow soil. The remaining area consists of valleys and low-lands with clay soil (Timouk et al., 2009). The Eguerit site is located on a rocky surface, whereas the Kelma site lies on a clay soil, covered by acacia forest (de Rosnay et al., 2009). The clay soil presents a low permeability to water, and the consequence of this feature is that Kelma site gets completely flooded during the wet season.

Figure 1: *Location of the flux sites. Coordinates : Eguerit Lon -1° 23' 24" Lat 15° 30' 0". Kelma Lon -1° 34' 12" Lat 15° 13' 12". Banizoumbou: Lon 2° 37' 48" Lat 13° 31' 12". Bellefongou: Lon 1° 43' 12" Lat 9° 47' 24".*

2.1.2. Banizoumbou site (Niger)

The studied area is located in the cultivated Sahelian environment of southwest Niger. The climate is semiarid with a potential evapotranspiration near 2500 mm yr^{-1} and a yearly mean rainfall of 570 mm. At the seasonal scale, 90% of the annual rainfall, mostly of convective origin, occurs from June to September. The natural vegetation is mainly woody savannah (dominant species: *Acacia* sp., *Balanites aegyptiaca*, *Prosopis* sp.) but under increasing land clearance most of the sandy slopes are now covered by a patchwork of fallow (dominated by *Guiera senegalensis*) and rain-fed millet fields. On the plateaus, the vegetation consists of the typically semiarid banded vegetation pattern of "tiger bush" (*Combretum micranthum*, *Combretum nigricans*, *Combretum glutinosum*, *Guiera senegalensis*). In the more clayey valley bottoms, the original bushy vegetation (*Piliostigma reticulatum*, *Bauhinia rufescens*, *Acacia* sp.) has now almost disappeared for cultivation of some specific water-demanding domestic crops (cassava, groundnut or sorghum) (Leblanc et al., 2008). The flux station is located in a millet field (Cappelaere et al., 2009)

2.1.3. Bellefoungou site (Benin)

Over this site, annual rainfall is 1200 mm, with 60% of the annual rainfall concentrated between July and September. The wet season extends from April to October. However, isolated rainfall can occur throughout the year, with the lowest probability during December and January. Natural vegetation is composed of a patchwork of dry forests and savannah, with dense and tall herbaceous strata, mainly composed of perennial grasses, and more or less dense woody strata. The original landscape has been modified by increasing cropping practices (Seghieri et al., 2009). The flux station is set over a clear forest. Trees are more than 10m high and less than 15m. They keep their leaves during the entire year except 2 months in December and January, but all species are not in phase. The surface characteristics are from loamy sand to sandy loam. An herbaceous strata grows between trees, being more dense where trees are more sparse. This forest site is quite different from the acacia forest of the Kelma site which is flooded during the wet season.

2.2. Data

2.2.1. Ground-based data

Net radiation data

All the sites were equipped with identical sensors to monitor the components of the net radiation at the surface (4-component sensor Kipp&Zonen CNR1 Radiation), except for the Bellefoungou site for which a NR-Lite sensor (for net long wave radiation) and two Skye pyranometers (for upward and downward solar radiation) were installed at 5m high. The albedo values used in this study were calculated from the ratio of the reflected to incident shortwave radiation provided by the sensors. The station was installed in an open area and the estimated albedo was not affected by shading except in the early morning and late afternoon.

Flux tower data

The sensible turbulent flux was measured by means of the eddy-covariance (EC) technique. The flux stations consisted of a three dimensional sonic anemometer (Model R3-50, Gill Solent Instruments, Lymington, UK) which provided measurements of the fluctuations of vertical velocity and air temperature. The sonic anemometer was controlled by a specially designed solid state logger (Center for Environment Hydrology, Wallingford, UK) which recorded the 20 Hz raw data and the 30 minute average of fluxes. More details of the complete installations and data processing can be found in Mougin *et al* (2009) for Eguerit and Kelma, in Ramier et al. (2009) for Banizoumbou and at the AMMA-CATCH website http://www.lthe.fr/catch/observation/measurement_doc/EF9_AE.H2OFlux_Odc_en.pdf for Bellefoungou. A detailed description of surface flux measurements for all sites can also be found in Lloyd and Taylor (2005).

2.2.2. Satellite data

The triangle method was applied using MODIS-Terra products. MODIS products are available freely for the science community which makes its use very attractive. Terra was the first EOS satellite launched, in December 18th, 1999, with MODIS as one of the five sensors onboard. The MODIS products used in this study were MOD11A1 (LST product) and MOD13A2 (Vegetation Indices). The current study was carried out at a regional scale, therefore the spatial resolution of 1 km provided by MODIS was considered adequate.

2.3. EF-retrieval method

The "triangle" method was first introduced by Price (1990) and later elaborated upon by Carlson et al. (1994; 1995), Moran et al. (1994), Gillies and Carlson (1995), Lambin and Ehrlich (1996), Owen et al. (1998), and Jiang and Islam (1999; 2001; 2003; 2004). This method was adopted and successfully applied to retrieve EF, ET and soil moisture by a number of researchers. Carlson (2007) gives an overview of the use of the "triangle" method for estimating ET and soil moisture. The basis of the methodology is the existence of a physically meaningful relationship between the evaporative fraction and a combination of remotely sensed spatial parameters, T_s (surface temperature) and NDVI (the Normalized Difference Vegetation Index). The scatter plot of T_s versus NDVI usually presents a triangle shape whose boundaries are interpreted as limiting surface fluxes, the upper limit being the warm edge and the lower limit being the cold edge. The version used in this study is the one proposed by Jiang and Islam (2001). The reader is referred to this paper and to Stisen et al. (2008) for the detailed description of the method.

2.4. Basis of the proposed parameterisation scheme

The evaporative fraction EF is defined as:

$$\mathrm{EF} = \lambda E/(R_\mathrm{n} - G) \qquad (2)$$

Expressing the ground heat flux as a function of net radiation

$$G = \alpha\, R_n \qquad (3)$$

and sensible heat flux

$$G = \gamma\, H \qquad (4)$$

and rearranging with Eqs. 1 and 2 supplies the following functional relationships between EF, α and γ:

$$\mathrm{EF} = 1 - \frac{1}{\gamma}\,\frac{\alpha}{1-\alpha} \qquad (5a)$$

$$\alpha = \frac{\gamma(1-\mathrm{EF})}{1 + \gamma(1-\mathrm{EF})} \qquad (5b)$$

$$\gamma = \frac{\alpha}{(1-\alpha)}\,\frac{1}{(1-\mathrm{EF})} \qquad (5c)$$

It should be noted that Eqs.5a, 5b and 5c are alternative – and equivalent - formulae to express the surface energy balance (Eq.1) in a non-dimensional form through EF, α and γ. Eq. 5a indicates that EF decreases with increasing α for a fixed γ value and increases with increasing γ for a fixed α value (Fig.2). Note that:

- for a given value of EF, there are several pairs of values (α, γ) that could be solution of the equation;
- for high positive values of γ, EF tends towards 1 and is practically insensitive to α;

- EF and α being positive during daytime , their values could be constrained within realistic lower and upper limits, whereas γ is not constrained – like the Bowen ratio - and could reach very high values (H $\approx$0) or could be negative (H<0) in case of local advective process (Fig. 2).

In this study, ground data were available of the ratio H/R_n , which is equal to α/γ:

$$\frac{H}{R_n} = \frac{H}{G} \times \frac{G}{R_n} = \frac{\alpha}{\gamma} \qquad (6)$$

We have therefore two equations (Eqs. 5 and 6) and three unknowns. It is necessary to make a plausible assumption about one of the unknowns to compute the two others. For the dry season, it was assumed that EF was equal to 0 (section 2.5). For the wet season, we used a plausible predetermined value of γ (section 2.6). Once the parameters were identified at each site (hereafter, with subscripts 'wet' and 'dry' respectively for the wet and dry season), they can be plotted in the EF-α (or EF-γ) space and used to derive a possible general relationship between the site-average values of EF and α - or γ - that can be used to predict G from EF. These seasonal values of EF, α and γ characterise the average energy balance at each site.

Figure 2: *Graphical representation of Eq. 5a showing the dependency of EF on α for different γ values. The two arrows represent plausible ranges for α at high (> 0.75) and low ($\approx$ 0) EF. Negative values of γ correspond to advective conditions (EF>1). The thick curve represents the relationship between EF and α for γ = 0.3. The parameter α was constrained to the interval 0<α<0.6.*

2.5. Parameter identification for the dry season

EF at the apogee of the dry season can be assumed to be equal to zero at the Sahelian sites (Banizoumbou, Eguerit and Kelma). For EF = 0, we get:

$$\gamma_{dry} = \frac{\alpha_{dry}}{1 - \alpha_{dry}} \tag{7a}$$

That is, as $H_{dry}/R_{n,dry} = \alpha_{dry}/\gamma_{dry}$, with $R_{n,dry}$ being the value of the net radiation observed at the time H_{dry} occurred, we get

$$\alpha_{dry} = 1 - (H_{dry}/R_{n,dry}) \tag{7b}$$

We calculated α_{dry} and γ_{dry} from the ground data sets for the 15 highest values of the ratio $H_{dry}/R_{n,dry}$ observed at 11h (MODIS-Terra overpass time) at the four sites and for sunny days of the dry season. The average value and standard deviation of the 15 values of α_{dry} and γ_{dry} at 11h were determined. For the semi-tropical site (Bellefoungou), evaporation during the dry season was small, yet not negligible and EF cannot be taken as 0. We therefore determined a proxy for EF_{dry} using the minimum value of EF provided by the triangle method (EF_{dry} ~0.15), and derived the corresponding values of α_{dry} and γ_{dry} at Bellegoungou, corresponding to the 15 highest values of $H_{dry}/R_{n,dry}$. The normalised difference vegetation index ($NDVI_{dry}$) and ground albedo (a_{dry}) and their standard deviations were calculated for the same days.

2.6. Parameter identification for the wet (monsoon) season

To identify the parameter values in the wet season, for which EF values were unknown, it was necessary to guess a plausible mean value of one of the two other unknowns, α or γ. Under high evapotranspiration rate, α is generally small, varying in the range $0<\alpha<0.10$. In this range, the assumption that γ is close to 0.30 might be quite realistic (Fig. 2). We therefore derived the instantaneous and mean values of EF and α using this assumption. In a similar way to the procedure applied for the dry season, we selected the 15 days with the lowest value of the ratio $H_{wet}/R_{n,wet}$, which were likely to correspond to the days with the highest evaporation fraction at each site.

2.7. Retrieved values of *H* and performance assessment

Replacing G by αR_n in the energy balance equation and rearranging, the retrieved values of H_r were obtained from:

$$H_r = (1-\alpha)(1-EF_T)R_n \tag{8}$$

where EF_T is the evaporative fraction retrieved by the triangle method.

The predictive performance of the different G–parameterisation schemes were assessed by means of the root mean square error (RMSE) and mean bias error (MBE) of the resulting retrieved values (H_r) with respect to the observed values (H_{obs}).

3. Results

3.1. Parameterisation of γ_{dry} and α_{dry}

Dry season

The average values of surface parameters (α_{dry}, γ_{dry}, $NDVI_{dry}$, a_{dry}) and fluxes ($R_{n,dry}$, H_{dry}, G_{dry}) at the four sites in the dry season are presented in Table 1. The average values of α_{dry} and γ_{dry}, varied in the interval [0.19-0.28] and [0.28-0.40], respectively, the highest value being found for Eguerit, the less vegetated site, with an average value of G_{dry} of 127 W m^{-2}, i.e. approximately 25-30% higher than the values found for the other sites ($G \approx 100$ W m^{-2}). The variability of α_{dry} and γ_{dry} was higher than that of NDVI and albedo, and the variability of G higher than that of H. The latter suggests that changes in R_n affected proportionally more G than H_s under dry conditions. The explanation might be that G depends mainly on T_s while H is driven by the surface–to-air temperature gradient, $T_s - T_a$, which is less sensitive than T_s to a change in R_n. Overall, the variation range and order of magnitude observed for α_{dry}, γ_{dry} and G were plausible.

Table 1: *Mean values of surface parameters (α_{dry}, γ_{dry}, $NDVI_{dry}$, a_{dry}) and fluxes ($R_{n,dry}$, H_{dry} , G_{dry}) at the four sites in the dry season. In parenthesis, standard deviation*

Wet season

In the wet season, the values of α_{wet} (assuming γ_{wet} =0.30) were found to vary in the interval [0.02-0.09] and EF_{wet} in the interval [0.68-0.94] (Table 2). As expected, the lowest values of H_{wet} and G_{wet} were observed at the Sudanian site (Bellefoungou) where the West African Monsoon is most intense, and at the Sahelian site of Kelma, subject to flooding. The highest values were observed at the Sahelian sites of Banizoumbou and Eguerit, where the Monsoon influence is substantially attenuated.

Table 2: *Mean values of surface parameters (α_{wet}, γ_{wet}, $NDVI_{wet}$ a_{wet}, EF_{wet}) and fluxes ($R_{n,wet}$, H_{wet} , G_{wet}) at the four sites in the wet season. In parenthesis, standard deviation.*

3.2. Representation in the EF-α space

When plotted in the EF-α space, the seasonal mean values of α showed a clear decreasing trend with increasing EF (Fig.3). A linear regression was fitted to these mean values, yielding the following empirical relationship between the site-averaged values of α and EF obtained for the dry and the wet season (R^2 = 0.96):

$$\alpha = -0.22\,\mathrm{EF} + 0.23 \qquad (10a)$$

Note that this relationship is close to the α - EF relationship provided by Eq. 5b for γ = 0.30 (Fig.3):

$$\alpha = \frac{0.3\,(1-\mathrm{EF})}{1 + 0.3\,(1-\mathrm{EF})} \qquad (10b)$$

In the following, Eq. 10a was used as the parameterisation formula linking α to EF

Figure 3: *Relationship α vs EF. Points are average-site values of the dry and wet season (Tables 1 and 2). The dashed line is the linear regression fitted to the points (Eq. 10a). The thick line (γ = 0.3) is Eq. 10b.*

3.3. Relationship between α and surface attributes (NDVI, a)

Plotting the site-average values of α against the corresponding average NDVI values (Fig. 4) revealed that there was no clear correlation between the two surface attributes. Rather, it was found a clear separation between the dry and wet seasons, with two clusters, one corresponding to high values of α and the other to low values. Therefore, α could not be accurately described over the whole range of EF when considering NDVI as the only explicative variable.

In the same figure, three formulae proposed in the literature are also shown:

- the linear function proposed by Su (2002):

$$\alpha = \alpha_0 + (\alpha_{max}-\alpha_0)\ (1-f_c) \qquad (11a)$$

where $\alpha_0 = 0.05$ and $\alpha_{max}=0.315$. The parameter f_c is the cover vegetation fraction computed as $f_c = (NDVI-NDVI_{min})^2/(NDVI_{max}-NDVI_{min})^2$, with $NDVI_{min} = 0.08$ (observed at Eguerit) and $NDVI_{max} = 0.86$ (observed at Bellefoungou).

- the formula of Bastiaanssen (2000)

$$\alpha = 0.20\ (1-0.96\ NDVI^4). \qquad (11b)$$

- the function proposed by Moran et al (1994)

$$\alpha = 0.583\ \exp(-2.13\ NDVI) \qquad (11c)$$

None of the above empirical formulae captured the annual changes in α, as shown by the two distinct clusters of points (Fig.4). Rather, it appears necessary to use two distinct equations for α, one for the dry season, and another one for the wet season.

Figure 4: *Evolution of α vs NDVI for the dry (open squares) and wet season (black circles). The dashed line is the function proposed by Moran et al., 1994: $\alpha = 0.583$ exp(-2.13 NDVI), the cross-line is the formula of Bastiaanssen et al. (2000) $\alpha = 0.20$ (1-0.96 NDVI^4). The continuous curve is the function proposed by Su (2002): $\alpha = \alpha_0 + (\alpha_{max}-\alpha_0)\ (1-f_c)$ where $\alpha_0 = 0.05$ and $\alpha_{max}=0.315$. f_c being the cover vegetation*

fraction computed as $f_c = (NDVI\text{-}NDVI_{min})^2/(NDVI_{max}\text{-}NDVI_{min})^2$, with $NDVI_{min} = 0.08$ (observed at Eguerit) and $NDVI_{max} = 0.86$ (observed at Bellefoungou).

Plotting the site-average values of α against the corresponding average albedo values (Fig. 5) led to the same conclusion as that drawn for NDVI, that is, there was a clear separation between the dry and wet seasons that cannot be accounted for by a unique relationship between α and surface albedo.

Figure 5: *Evolution of α vs albedo for the dry (open squares) and wet (black circles) season.*

3.4. Performance assessment of the parameterization schemes

A total of 451 retrieved values of H from MODIS-Terra overflights throughout the years 2005-2007 at the four sites were used to assess the performance of the new parameterisation scheme combined to the triangle method. Our ground reference values were the observed values of H (H_{obs}) obtained from the flux-tower measurements. The values of retrieved sensible flux, were calculated by means of Eq. 8, using the observed values of R_n, $R_{n,obs}$. The calculations were performed for four different parameterizations of G:

- Par-1: G was estimated from the relationship α vs EF established in this study and given by Eq. 10a;
- Par-2; G was calculated following Su (2002), with α linked to the cover fraction, f_c, through Eq. 11a;

- Par-3: G was predicted from the formula proposed by Bastiaanssen (2000), (Eq. 11b);
- Par-4: G was estimated from the formula proposed by Moran et al (1994), with α given by Eq. 11c.

The values of the statistical estimators RMSE and MBE of the relationship H_r vs H_{obs} (Table 3) indicated that there was a clear improvement of the predictions when using Par-1 for all sites, with respect to the VI-based parameterisation (Par-2 to Par-4). Among the latter, Par-3 was performing the best. Pooling the data of all sites, RMSE was 41.5 W m^{-2} and MBE was -11.2 W m^{-2} for Par-1, compared to 65.5W m^{-2} and -51.3 W m^{-2} for Par-2, 50.4 and -25.1 W m^{-2} for Par-3 and 83.7 and -65.1 W m^{-2} for Par-4. To highlight the negative bias occurring in all the sites, the regression H_r vs H_{obs}, using the best-performing parameterisation (Par-1) is presented in Figure 6 together with the regression lines. Underestimation of H occurred mainly in the upper range (H > 300 W m^{-2}).

Table 3: *Statistical estimators (RMSE and MBE, in W m^{-2}) of the regression analysis between H_r and H_{obs}*

Figure 6*. Comparison between retrieved (using Par-1) and observed sensible heat flux for (a) Banizoumbou (b) Eguerit (c) Kelma (d) Bellefoungo (e) all sites (pooled data). Dashed lines = linear regression, dotted lines = 1:1 relationship.*

The H_r and λE_r mean relative difference of the VI-based formulae with respect to the EF-based formula highlighted a general underestimation of the VI-formulae (Table 4).

The smallest differences with Par-1 were found for Par-3 (-10% and -8% respectively for H_r and λE_r). The reason for the relatively close agreement between Par-1 and Par-3 predictions could stay in that (i) Par-3 predicted similar values of α as Par-1 for the dry season (Fig.4) and (ii) differences in α for the wet season were not very critical when retrieving ET at high EF because of the small relative weight of the ground heat flux in the energy balance. This result underlined that a realistic estimation of the value of α in the dry season is one of the main requirements to get reliable values of the other terms of the energy balance in semi-arid regions.

Table 4: *Mean values (W m^{-2}) of retrieved fluxes (G, H and λE) and relative mean differences (RMD, %) of VI-based values (Par-2, Par-3, Par-4) with respect to the values supplied by Par-1*

~~The estimated values of α obtained from Par-1 presented a significant level of correlation with NDVI (R^2 = 0.44). This result indicated that Par-1 was able to include – at least partially – the influence of NDVI on the ground heat flux~~.

4. Discussion

4.1. Performance of the EF-based parameterisation

Our study confirmed the general validity and reliability of the triangle method (Jiang and Islam, 2001; Batra et al., 2006; Stisen et al., 2008), and its robustness. The statistical estimators RMSE and MBE obtained with Par-1 for the sensible flux were about 40 Wm^{-2} and -10 Wm^{-2}, respectively (Table 3). This is an acceptable performance when compared with the range of errors quoted for the latent flux λE. Kalma et al. (2008) performed a reanalysis of 30 published validations to estimate λE

from remote sensing, and showed that the average RMSE was about 50 W/m^2, ranging from 20 to 132 W/m^2. The errors obtained in the current study were also similar to other validation studies using the triangle method carried out for different sites and satellites' sensors, such as Southern Great Plains in the US with AVHRR and MODIS (Jiang and Islam, 2001; Batra et al., 2006) or Northern Senegal in Western Africa with MSG-SEVIRI sensor (Stisen et al., 2008)

However, the difficulty in 'guessing' the wet edge in absence of fully wet pixels may lead to large uncertainties. This appears to be the main limitation of the method under dry and arid climates, as highlighted in this study by the systematic underestimation of H - and therefore, overestimation of λE - under very dry conditions (H> 300 W m^{-2}) and for all sites (Fig. 6). The underestimation was especially strong for Eguerit (Fig. 6b) where almost all the predicted values were underestimated, with some errors reaching -150 W/m^2. Note that Eguerit is the driest and the less vegetated of the four sites, and that the triangle method is especially prone to significant errors in determining the wet edge of the LST-NDVI space in very dry areas lacking of 'wet' pixels. The highest deviations could therefore be attributed to the retrieval algorithm rather than to the parameterisation approach of the soil heat flux.

4.2. Advantages and limitations of the EF-based parameterisation

The parameterisation scheme proposed in this work has the important advantage of being simple to apply, to be parsimonious in input requirements and to be based on a robust hypothesis, the decrease of G and H with increasing EF (i.e. with increasing soil moisture and/or vegetation cover). The method could potentially be applied to any semi-arid area with contrasted dry and wet seasons. Another advantage of the EF-based parameterisation is that EF includes the effects of the prevailing weather conditions and soil moisture regime at satellite overpass, whereas vegetation indices are varying slowly, and cannot account for sudden changes in weather or in recent rainfalls that modify the soil water status. In other words, EF captures the effect of rapid changes in aerial environment and soil moisture while vegetation indices respond to these changes with a large delay. This is the main argument in favour of the EF-based parameterisation

Our results also indicated that the choice of a vegetation index (NDVI, *f*c) as predictor of α is likely to be the main cause of the relatively poor performance of the VI-based formulae (Table 3). The reason is that VIs cannot account for the contrasted soil moisture regimes of the dry and wet seasons. A possible recommended option would be to use two distinct α-VI relationships, one for the dry season and the other one for the wet season.

It has been recognised several limitations inherent to the choice of R_n as predictive variable. Santanello and Friedl (2003) and Murray and Verhoef (2007a,b), among others, pointed out that G vs R_n relationships cannot account for the dependency of G on soil moisture and ignore the asymmetry in the diurnal variation of G relative to R_n. With the new parameterisation, the first drawback was minimised as α was expressed as a function of EF, which implicitly accounts for soil moisture and evaporation. The second drawback - asymmetry between G and R_n - implies that the proposed parameterisation (e.g. Eq. 10a or 10b) would be valid only at the overpass time of MODIS-Terra. Applying the same equation to other hours of the day might be hazardous, as a lag exists between G and H which peaks at different hours (Santanello and Friedl, 2003).

To elucidate this point, we calculated the values of α_{dry} at the four sites for each hour of the period from 9:00 to 15:00, in the same way we did for the Modis-Terra overpass time (Section 2.5). The results (Figure 7) showed that, during the dry season, the parameter α_{dry} decreased from a maximum in the early morning (09:00) towards lower values or even negative values in the mid-afternoon hours.

Figure 7: *Values of α_{dry} for each hour of the period 9.00 to 15.00 h. Symbols: circles = Bellefoungou; squares = Kelma; triangles = Eguerit; diamond =Bani. The curves are the best fit of Eq. 12 (SF-model) to the points.*

The decreasing trend was well described by the empirical model proposed by Santanello and Friedl (2003), hereafter noted SF:

$$\alpha = A\,cos\left[\frac{2\pi(t+10800)}{B}\right] \qquad (12)$$

where t is time of day in seconds (t = 0 at solar noon). The coefficients A (i.e., the maximum value of α) and B (indicative of the time lag between G and H) are adjusting factors which were set at 0.31 and 74,000 s respectively in the original SF-model. This relationship has been proven to provide improvement to estimated values of G (Chehbouni et al., 2008).

The SF- model adjustment was performed only for the dry season, for which α_{dry} could be determined with reasonable accuracy from the procedure described in 2.5. For the wet season, the high uncertainty and relative errors on α_{wet} and its small range of variation prevent the same type of exercise. The best fit values of the parameters for the dry season (A_{dry} and B_{dry}) at the four sites, by minimising model RMSE are presented in Table 5. The A_{dry} values ranged in the interval [0.24-0.35], with the lowest value found at the semi-tropical site (Bellefongou) and the highest value at the driest site (Eguerit). The coefficient B_{dry} varied in the interval [75000 - 96500], with the lowest value for Bellefongou and the highest value for Kelma (acacia forest site). Both coefficients – especially A_{dry} - were well correlated with $NDVI_{dry}$ (Fig. 8a-b), and could be predicted by means of the following linear relationships:

$$A_{dry} = -0.31\ NDVI_{dry} + 0.37 \qquad R^2 = 0.86 \qquad (13)$$

$$B_{dry} = -50900\ NDVI_{dry} + 97160 \qquad R^2 = 0.65 \qquad (14)$$

The SF-model combined with Eqs. 13 and 14 supplied a fair prediction of α (Fig.8) and could be considered as a robust alternative to estimate α from NDVI when EF is very small (e.g., EF < 0.1).

Figure 8: *Relationship between observed (α_{obs}) and estimated (α_{est}) values of $\alpha = G/R_n$. Estimates from the SF-model with A_{dry} and B_{dry} given by Eqs. 13 and 14. The line is the linear regression $\alpha_{est.} = 0.96\ \alpha_{obs} + 0.01$ ($R^2 = 0.94$, RMSE = 0.029)*

Overall, the latter results reconciled partly the VI- and EF-based schemes. We demonstrated that the VI-based scheme could be applied for the dry season through a specific parameterisation of the SF-model. It is very likely that this parameterisation would not be valid for the whole year (see Fig.4) and that a specific parameterisation of the SF-model should be searched for the wet season. The latter suggests that surface moisture rather than VI is the primary factor that drives the annual trend of α. As the EF-scheme accounts for the surface moisture through EF, it can be applied over the whole year, independently of the season.

To conclude, our EF-based parameterisation scheme, applicable to the whole range of EF, appears more robust than other existing empirical methods as it implicitly includes the effect of soil moisture and soil properties. It also relies on a more solid theoretical basis as we established that α is functionally related to EF. Besides, it was demonstrated that, under dry surface conditions (lower range of EF), the diurnal asymmetry between G and R_n at each site could be accounted for by linking the coefficients of the SF-model to NDVI.

These parameterisations provide empirical but practical alternatives to the universal but more complex method based on solving the physically-based equations that describe the process of soil heat conduction. The choice between the two approaches should be made in function of the available input data on physical properties and water status of the soil, keeping in mind that the empirical approach is much less demanding in input data and computational process than the physically-based approach.

Acknowledgements

The data used in this study were obtained in the frame of the AMMA (African Monsoon Multidisciplinary Analysis) programme, which is currently funded by a large number of agencies, especially from France, UK, US and Africa, and of the French AMMA-Catch observing system. In the last years, AMMA has been granted by a major financial support from the European Community's Sixth Framework Research Programme (AMMA-EU Integrated Project). Detailed information on objectives, teams, data and results is available on the AMMA International web site (http://www.amma-international.org.) and the AMMA-Catch observation system (www.amma-catch.org).

References

Allen, R.G., Pereira, L.S., Raes, D., & Smith, M. (1998). Crop evapotranspiration - Guidelines for computing crop water requirements - FAO Irrigation and drainage paper 56. Rome: Food and Agriculture Organization of the United Nations, xxvi, 300 p.: ill. ; 30 cm, ISBN: 9251042195.

Bastiaanssen, W.G.M., Menenti, M., Feddes, R. A., & Holtslag, A.A.M. (1998a). A remote sensing surface energy balance algorithm for land (SEBAL). 1. Formulation. Journal of Hydrology, 212/213, pp. 198-212.

Bastiaanssen, W.G.M., Pelgrum, H., Wang, J., Ma, Y., Moreno, J.F., Roeking, G.J., & Van der Wal, T. (1998b). A remote sensing surface energy balance algorithm for land (SEBAL). 2. Validation. Journal of Hydrology, 212/213, pp. 213-229.

Bastiaanssen, W.G.M (2000). SEBAL-based sensible and latent heat fluxes in the irrigated Gediz Basin, Turkey. Journal of Hydrology, 229, pp. 87-100.

Batra, N., Islam, S., Venturini, V., Bisht, G., & Jiang, L. (2006) Estimation and comparison of evapotranspiration from MODIS and AVHRR sensors for clear sky days over the Southern Great Plains. Remote Sensing of Environment, 103, pp. 1-15.

Berkowicz, R., and Prahm (1982). Sensible heat flux estimated from routine meteorological data by the resistance method. Journal of Applied Meteorology, 21, pp. 1845–1864.

Bisht, G.; Venturini, V.; Islam, S., and Jiang, L. (2005). Estimation of the net radiation using MODIS (Moderate Resolution Imaging Spectroradiometer) data for clear sky days. Remote Sensing of Environment, 97, pp. 52-67.

Boken, V.K. (2009). Improving a drought early warning model for an arid region using a soil-moisture index. Applied Geography, 29, pp 402-408.

Brutsaert, W. (1982). Evaporation into the atmosphere. Kluwer Academic Publishers, ISBN: 90-277-1247-6

Bhumralkar, C. (1975). Numerical experiments on the computation of ground surface temperature in an atmospheric general circulation model. Journal of Applied Meteorology, 14, pp. 1246-1258

Cappelaere B., Descroix L., Lebel T., Boulain N., Ramier D., Laurent J.P., Favreau G., Boubkraoui S., Boucher M., Moussa I.B., Chaffard V., Hiernaux P., Issoufou H.B.A., Le Breton E., Mamadou I., et al. (2009). The AMMA-CATCH experiment in the cultivated Sahelian area of south-west Niger - Investigating water cycle response to a fluctuating climate and changing environment. Journal of Hydrology, 375(1-2), 34-51.

Carlson, T.N., Gillies, R.R., and Perry, E.M. (1994). A Method to Make Use of Thermal Infrared Temperature and NDVI measurements to Infer Surface Soil Water Content and Fractional Vegetation Cover. Remote Sensing Reviews, 9, pp. 161-173.

Carlson, T.N., Gillies, R.R., and Schmugge, T.J. (1995) An Interpretation of Methodologies for Indirect Measurement of Soil-Water Content. Agricultural and Forest Meteorology, 77, pp. 191-205.

Carlson, T. (2007). An Overview of the "Triangle Method" for Estimating Surface Evapotranspiration and Soil Moisture from Satellite Imagery. Sensors, 7, pp. 1612-1629.

Cellier, P., Richard, G., and Robin, P. (1996). Partition of sensible heat fluxes into bare soil and the atmosphere. Agricultural and Forest Meteorology, 82, pp. 245–265.

Chehbouni, A., Hoedjes, J.C.B., Rodriquez, J.C., Watts, C.J., Garatuza, J., Jacob, F., and Kerr, Y.H. (2008). Using remotely sensed data to estimate area-averaged daily surface fluxes over a semi-arid mixed agricultural land. Agricultural and Forest Meteorology, 148, pp. 330-342.

Choudhury, B. J. (1987). Relationships between vegetation indices, radiation absorption, and net photosynthesis evaluated by a sensitivity analysis. Remote Sensing of Environment, 22, pp. 209–233.

Courault D., Seguin B. and Olioso A. (2005). Review on estimation of evapotranspiration from remote sensing data: From empirical to numerical modeling approaches. Irrigation and Drainage Systems, 19, 223-249.

Crawford, T. M.; Stensrud, D. J.; Carlson, T. N., and Capehart, W. J. (2000). Using a soil hydrology model to obtain regionally averaged soil moisture values. Journal of Hydrometeorology, 1, pp. 353–363.

Deardorff, J. (1978). Efficient prediction of ground surface temperature and moisture, with inclusion of a layer of vegetation. Journal of Geophysical Research, 83, pp. 1889–1903.

De Rosnay, P.; Gruhier, C.; Timouk, F.; Baup, F.; Mougin, E.; Hiernaux, P.; Kergoat, L., and LeDantec, V. (2009). Multi-scale soil moisture measurements at the Gourma meso-scale site in Mali. Journal of Hydrology, 375, pp. 241-252.

Frappart, F.; Hiernaux, P.; Guichard, F..; Mougin, E.; Kergoat, L.; Arjounin M.; Lavenu, F.; Koité, M.; Paturel, J.-E.; Lebel, T.; (2009). Rainfall regime across the Sahel band in the Gourma region, Mali. Journal of Hydrology, 375, pp. 128-142.

Friedl, M.A. (2002). Forward and inverse modelling of land surface energy balance using surface temperature measurements. Remote Sensing of Environment, 79, pp. 344–354.

Gillies, R.R., and Carlson, T.N. (1995) Thermal Remote Sensing of Surface Soil Water Content with Partial Vegetation Cover for Incorporation into Climate Models. Journal of Applied Meteorology, 34, 745-756.

Hellegers, P.J.G.J., Soppe, R., and Perry, C.J. (2009). Remote Sensing and Economic Indicators for Supporting Water Resources Management Decisions. Water Resources Management, 24, 2419-2436.

Humes, K. S., Kustas, W. P., and Moran, M. S. (1994). Use of remote sensing and reference site measurements to estimate instantaneous surface energy balance components over a semiarid rangeland watershed. Water Resources Research, 30, pp. 1363-1373.

Jacobsen, A., and Hansen B.U. (1999). Estimation of the soil heat flux/net radiation ratio based on spectral vegetation indexes in high-latitude Artic areas. International Journal of Remote Sensing, 20, pp. 445–461.

Jiang, L., and Islam, S. (1999). A Methodology for Estimation of Surface Evapotranspiration over Large Areas using Remote Sensing Observations. Geophysical Research Letters, 26, pp. 2773-2776.

Jiang, L., and Islam, S. (2001). Estimation of Surface Evaporation Map Over Southern Great Plains Using Remote Sensing Data, Water Resources Research, 37, pp. 329–340.

Jiang, L., and Islam, S. (2003). An Intercomparison of Regional Latent Heat Flux Estimation using Remote Sensing Data. International Journal of Remote Sensing, 24, pp. 2221-2236.

Jiang, L., Islam, S., and Carlson, T.N. (2004). Uncertainties in latent heat flux measurement and estimation: implications for using a simplified approach with remote sensing data. Canadian Journal of Remote Sensing, 30, pp. 769-787.

Kalma, J.D., McVicar, T.R., and McCabe, M.F. (2008). Estimating Land Surface Evaporation: A Review of Methods Using Remotely Sensed Surface Temperature Data. Surveys in Geophysics, 29, 421-469.

Kergoat, L., Grippa, M., Baille, A., Eymard, L., Lacaze, R., Mougin, E., Ottlé, C., Pellarin, T., Polcher, J., De Rosnay, P., Roujean, J-L., Sandholt, I., Taylor, C.M., Zin,I., and Zribi, M. (2011). Remote sensing of the Land Surface during the African Monsoon Multidisciplinary Analysis (AMMA). Atmospheric Science Letters, 12, pp. 129-134.

Kustas, W. P., and Daughtry, C. S. T. (1990). Estimation of the Soil Heat Flux/Net Radiation Ratio from Spectral Data. Agricultural and Forest Meteorology, 49, pp. 205-223

Kustas, W. P. and Goodrich, D. C. (1994). Preface. Water Resources Research, 30, pp. 1211–1225.

Kustas, W.P., Daughtry, C.S.T., and van Oevelen, P.J. (1993). Analytical treatment of the relationships between soil heat flux/net radiation ratio and vegetation indices. Remote Sensing of Environment, 46, pp. 319–330.

Lambin, E.G., and Ehrlich, D. (1996). The Surface Temperature-vegetation Index Space for Land Cover and Land-cover Change Analysis. International Journal of Remote Sensing, 17, pp. 463-487.

Lebel, T., Cappelaere, B., Galle, S., Hanan, N., Kergoat, L., Levis, S. Vieux, B., Descroix, L-, Gosset, M., Mougin, E:, Peugeot, C., Seguis, L. (2009). AMMA-CATCH studies in the Sahelian region of West-Africa: An overview. Journal of Hydrology, 375, pp. 3–13

Leblanc, M.J.; Favreau, G.; Massuel, S.; Tweed, S.O.; Loireau, M., and Cappelaere, B. (2008). Land clearance and hydrological change in the Sahel: SW Niger. Global and Planetary Change, 61, pp. 135-150.

Li, Z.L., Tang, R., Wan, Z., Bi, Y., Zhou, C., Tang, B., Yan, G., and Zhang, X. (2009). A Review of Current Methodologies for Regional Evapotranspiration Estimation from Remotely Sensed Data. Sensors, 9, pp. 3801-3853.

Liebethal, C., and Foken, T. (2007). Evaluation of six parameterization approaches for the ground heat flux. Theoretical and Applied Climatology, 88, pp. 43-56.

Lloyd, C., and Taylor, C. (2005). EOP Surface Flux Measurements TT2a. In Medias-France (Eds.), AMMA International Implementation Plan version 2.0, Chapter 3 (pp. 1-17), E-publishing. http://amma.mediasfrance.org/implementation/docs/TT2a.pdf

McCabe, M.F., and Wood, E.F. (2006). Scale influences on the remote estimation of evapotranspiration using multiple satellite sensors. Remote Sensing of Environment, 105, pp. 271-285.

Mecikalski, J. R.; Diak, G. R.; Anderson, M. C., and Norman, J. M. (1999). Estimating fluxes on continental scales using remotely sensed data in an atmospheric–land exchange model. Journal of Applied Meteorology, 38, pp. 1352–1369.

Moran, M.S.; Clarke, T.R.; Inoue, Y., and Vidal, A. (1994). Estimating crop water deficit using the relation between surface-air temperature and spectral vegetation index. Remote Sensing Environment, 49, pp. 246–263.

Mougin, E., Hiernaux, P., Kergoat, L., Grippa, M., de Rosnay, P., Timouk, F., Le Dantec, V., Demarez, V., Lavenu, F., Arjounin, M., Lebel, T., Soumaguel, N., Ceschia, E., Mougenot, B., Baup, F., Frappart, F., Frison, P.L., Gardelle, J., Gruhier, C., Jarlan, L., Mangiarotti, S., Sanou, B., Tracol, Y., Guichard, F., Trichon, V., Diarra, L., Soumaré, A., Koité, M., Dembélé, F., Lloyd, C., Hanan, N.P., Damesin, C., Delon, C., Serça, D., Galy-Lacaux, C., Seghieri, J., Becerra, S., Dia, H., Gangneron, F., and P. Mazzega (2009). The AMMA-CATCH Gourma observatory site in Mali: Relating climatic variations to changes in vegetation, surface hydrology, fluxes and natural resources. Journal of Hydrology, 375, pp. 14-33.

Mu, Q.; Heinsch, F.A.; Zhao, M., and Running, S.W. (2007). Development of a global evapotranspiration algorithm based on MODIS and global meteorology data. Remote Sensing of Environment, 111 pp. 519-536.

Murray, T., and Verhoef, A. (2007a). Moving towards a more mechanistic approach in the determination of soil heat flux from remote measurements: I. A universal approach to calculate thermal inertia. Agricultural and Forest Meteorology, 147, pp. 80-87.

Murray, T., and Verhoef, A. (2007b). Moving towards a more mechanistic approach in the determination of soil heat flux from remote measurements. Part II. Diurnal shape of soil heat flux. Agricultural and Forest Meteorology, 147, pp. 88–97.

Nishida, K.; Nemani, R.R.; Running, S.W., and Glassy, J.M. (2003). An operational remote sensing algorithm of land surface evaporation, Journal of Geophysical Research-Atmospheres 108, pp. 4270.

Norman, J.M.; Kustas, W.P., and Humes, K.S. (1995). A two-source approach for estimating soil and vegetation energy fluxes from observations of directional radiometric surface temperature. Agricultural and Forest Meteorology, 77, pp. 263-293.

Norman, J. M.; Kustas, W. P.; Prueger, J. H., and Diak, G. R. (2000). Surface flux estimation using radiometric temperature: A dual-temperature-difference method to minimize measurement errors. Water Resources Research, 36, pp.2263–2274.

Nuñez, C.M., Varas, E.A., and Meza, F.J. (2010). Modelling soil heat flux. Theoretical and Applied Climatology, 100, pp. 251-260

Ochsner, T.E., Sauer, T.J., and Horton, R. (2006). Field Tests of the Soil Heat Flux Plate Method and Some Alternatives. Agronomy Journal, 98, pp.:1005–1014

Owen, T.W.; Carlson, T.N., and Gillies, R.R. (1998). An Assessment of satellite Remotely-sensed Land Cover Parameters in Quantitatively Describing the Climatic Effect of Urbanization. International Journal of Remote Sensing, 19, pp. 1663-1681.

Price, J.C. (1990) Using spatial context in satellite data to infer regional scale evapotranspiration. IEEE Transactions on Geoscience and Remote Sensing, 28, 940–948.

Ramier, D., Boulain, N., Cappelaere, B., Timouk, F., Rabanit, M., Lloyd, C.R., Boubkraoui, S., Métayer, F., Descroix, L., and Wawrzyniak, V. (2009). Towards an understanding of coupled physical and biological processes in the cultivated Sahel – 1. Energy and water. Journal of Hydrology, 375, pp. 204-216.

Roerink, G.J.; Su, Z., and Menenti, M. (2000). S-SEBI: A simple remote sensing algorithm to estimate the surface energy balance. Physics and Chemistry of the Earth. Part B: Hydrology, Oceans and Atmosphere, 25, pp.147–157.

Santanello, J.A., and Friedl, M.A. (2003). Diurnal covariation in soil heat flux and net radiation. Journal of Applied Meteorology, 42, pp. 851–862.

Seghieri, J.; Vescovo, A.; Padel, K., Soubie, R.; Arjounin, M.; Boulain, N.; de Rosnay, P.; Galle, S.; Gosset, M.; Mouctar, A.H.; Peugeot, C., and Timouk, F. (2009). Relationships between climate, soil moisture and phenology of the woody cover in two sites located along the West African latitudinal gradient. Journal of Hydrology, 375, pp. 78-89.

Schüttemeyer, D., Moene, A. F., Holtslag, A. A. M., de Bruin, H. A. R., and Van de Giesen, N. (2006). Surface Fluxes and Characteristics of Drying Semi-Arid Terrain in West Africa. Boundary-Layer Meteorology, 118, pp. 583-612

Scott, R.L. (2010). Using watershed water balance to evaluate the accuracy of eddy covariance evaporation measurements for three semiarid ecosystems. Agricultural and Forest Meteorology, 150, pp. 219-225.

Stisen, S.; Sandholt, I.; Nørgaard, A.; Fensholt, R., and Jensen K.H. (2008). Combining the triangle method with thermal inertia to estimate regional evapotranspiration – Applied to MSG-SEVIRI data in the Senegal River basin. Remote Sensing of Environment, 112, pp. 1242-1255.

Su, Z. (2002). The Surface Energy Balance System (SEBS) for estimation of turbulent heat fluxes. Hydrology and Earth System Sciences, 6, pp. 85–99.

Tang, R.; Li, Z.L., and Tang, B. (2010). An application of the Ts–VI triangle method with enhanced edges determination for evapotranspiration estimation from MODIS data in arid and semi-arid regions: Implementation and validation. Remote Sensing of Environment, 114, pp. 540-551.

Timouk, F.; Kergoat, L.; Mougin, E.; Lloyd, C.R.; Ceschia, E.; Cohard, J.-M.; de Rosnay, P.; Hiernaux, P.; Demarez, V., and Taylor, C.M. (2009). Response of surface energy balance to water regime and vegetation development in a Sahelian landscape. Journal of Hydrology, 375, pp. 178-189.

Verhoef, A., Ottlé, C., Cappelaere, B., Murray, T., Saux-Picart, S., Zribi, M., F., Maignan, Boulain, N., Demarty, and J., Ramier, D. (2012). Spatio-temporal surface soil heat flux estimates from satellite data; results for the AMMA experiment at the Fakara (Niger) supersite. Agricultural and Forest Meteorology, 154-155, pp. 55-66.

Verstraeten, W.W.; Veroustraete, F., and Feyen, J. (2008). Assessment of Evapotranspiration and Soil Moisture Content Across Different Scales of Observation. Sensors, 8, pp. 70-117.

Wang, J., and Bras, R.L. (1999). Ground heat flux estimated from surface soil temperature. Journal of Hydrology, 216, pp. 214-226

Wang, Z.H., and Bou-Zeid, E. (2012). A novel approach for the estimation of soil ground heat flux. Agricultural and Forest Meteorology, 154-155, pp. 214-221

Zschau, J., and A. N. Küppers (2003), Early Warning Systems for Natural Disaster Reduction, 834 pp., Springer, Berlin. ISBN 3540679626

Table 1: Mean values of surface parameters (α_{dry}, γ_{dry}, $NDVI_{dry}$, a_{dry}) and fluxes ($R_{n,dry}$, H_{dry} , G_{dry}) at the four sites in the dry season. In parenthesis, standard deviation

Site	α_{dry}	γ_{dry}	$NDVI_{dry}$	a_{dry}	$R_{n,dry}$ (W m^{-2})	H_{dry} (W m^{-2})	G_{dry} (W m^{-2})	EF_{dry} (fixed)
Banizoumbou	0.24 (±0.06)	0.31 (±0.10)	0.16 (±0.01)	0.37 (±0.02)	407 (±24)	321 (±19)	97 (±26)	0
Eguerit	0.25 (±0.11)	0.36 (±0.19)	0.11 (±0.02)	0.23 (±0.03)	485 (±65)	359 (±13)	127 (±39)	0
Kelma	0.19 (±0.0.04)	0.24 (±0.06)	0.16 (±0.03)	0.19 (±0.03)	504 (±16)	408 (±19)	96 (±23)	0
Bellefoungou	0.22 (±0.12)	0.36 (±0.23)	0.42 (±0.05)	0.20 (±0.03)	479 (±43)	310 (±22)	106 (±29)	0.15

Table 2: Mean values of surface parameters (α_{wet}, γ_{wet}, $NDVI_{wet}$ a_{wet}, EF_{wet}) and fluxes ($R_{n,wet}$, H_{wet} , G_{wet}) at the four sites in the wet season. In parenthesis, standard deviation

Site	α_{wet}	γ_{wet} (fixed)	$NDVI_{wet}$	a_{wet}	$R_{n,\ wet}$ (W m^{-2})	H_{wet} (W m^{-2})	G_{wet} (W m^{-2})	EF_{wet}
Banizoumbou	0.05 (±0.01)	0.30	0.29 (±0.01)	0.30 (±0.02)	581 (±23)	95 (±27)	28 (±84)	0.83 (±0.04)
Eguerit	0.09 (±0.02)	0.30	0.11 (±0.02)	0.22 (±0.02)	475 (±110)	141 (±48)	42(±14)	0.68 (±0.07)
Kelma	0.02 (±0.01)	0.30	0.56 (±0.03)	0.09 (±0.01)	802 (±50)	49(±26)	15 (±8)	0.94 (±0.03)
Bellefoungou	0.07 (±0.01)	0.30	0.58 (±0.13)	0.15 (±0.01)	689 (±74)	162 (±30)	49 (±9)	0.75 (±0.04)

Table 3: Statistical estimators (RMSE and MBE, in W m^{-2}) of the regression analysis between H_r and H_{obs}

	Par-1 (Eq. 10a)		Par-2 (Eq. 11a)		Par-3 (Eq.11b)		Par-.4 (Eq.11c)	
Site	RMSE	MBE	RMSE	MBE	RMSE	MBE	MBE	MBE
Banizoumbou	37.6	0.5	52.8	-37.7	41.2	-14.5	70.6	-47.3
Eguerit	41.3	-4.3	69.8	-58.3	47.9	-29.9	106.8	-58.3
Kelma	41.4	-33.9	86.6	-77.3	56.9	-51.5	105.3	-90.3
Bellefoungo	48.5	-22.4	70.8	-56	59.6	-42.5	62.7	-34.7
All sites	*41.5*	*-11.2*	*65.5*	*-51.3*	*50.4*	*-25.1*	*83.7*	*-65.1*

Table 4: Mean values (W m^{-2}) of retrieved fluxes (G, H and λE) and relative mean differences (RMD, %) of VI-based values (Par-2, Par-3, Par-4) with respect to the values supplied by Par-1

	Par-1 (Eq.10a)	Par-2 (Eq.11a)		Par-3 (Eq.11b)		Par-4 (Eq.11c)	
	Mean	Mean	RMD	Mean	RMD	Mean	RMD
G	52.4	124.0	′+137%	90.9	+74%	159.0	+204%
H	217.1	176.3	-19%	199.1	-10%	166.4	-25%
λE	199.6	168.7	-19%	179.1	-8%	159	-26%

Table 5: Values of the parameters A_{dry} and B_{dry} (Eq. 12) and model RMSE at the four sites

Site	A	B	RMSE
Banizoumbou	0.29	86500	0.017
Eguerit	0.35	88000	0.028
Kelma	0.32	96500	0.017
Bellefoungou	0.24	75000	0.024

Figure 1: *Location of the flux sites. Coordinates : Eguerit Lon -1° 23' 24" Lat 15° 30' 0". Kelma Lon -1° 34' 12" Lat 15° 13' 12". Banizoumbou: Lon 2° 37' 48" Lat 13° 31' 12". Bellefongou: Lon 1° 43' 12" Lat 9° 47' 24".*

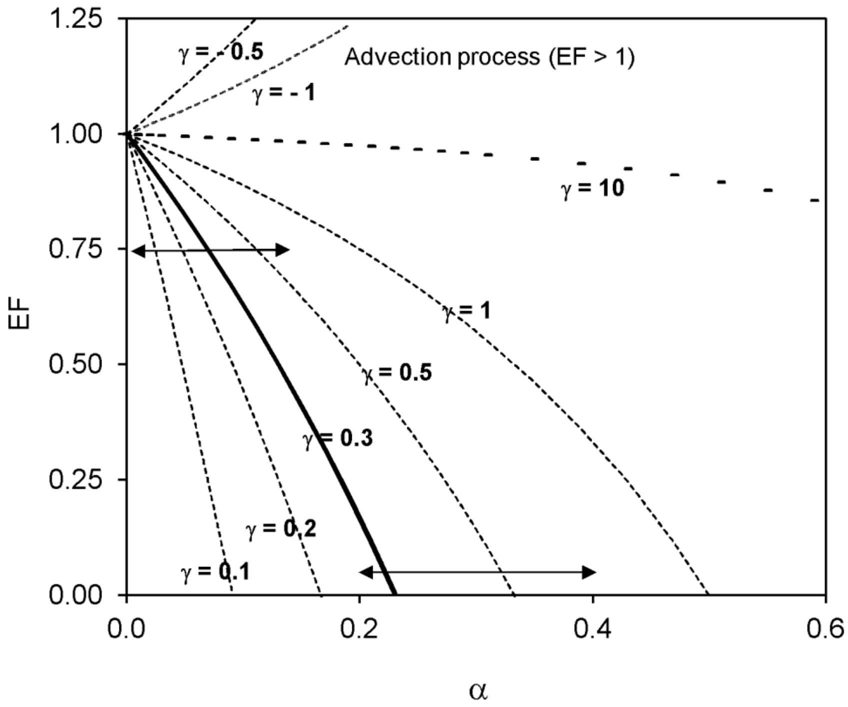

Figure 2: *Graphical representation of Eq. 5a showing the dependency of EF on α for different γ values. The two arrows represent plausible ranges for α at high EF (EF > 0.75) and low EF (EF $\approx$ 0). Negative values of γ correspond to advective conditions (EF>1). The thick curve represents the relationship between EF and α for γ = 0.3. The parameter α was constrained to the interval $0<\alpha<0.6$.*

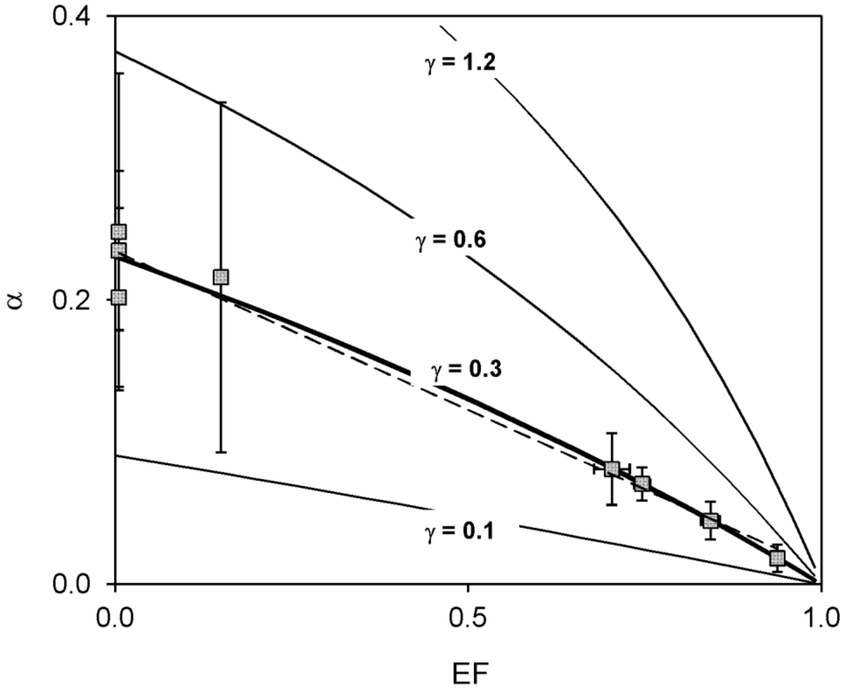

Figure 3: *Relationship α vs EF. Points are average-site values of the dry and wet season (Tables 1 and 2). The dashed line is the linear regression fitted to the points (Eq. 10a). The thick line (γ = 0.3) is Eq. 10b.*

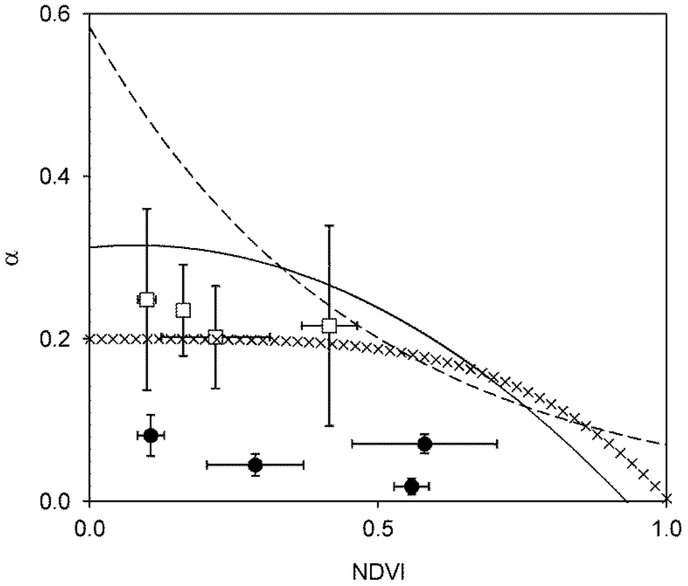

Figure 4: *Evolution of α vs NDVI for the dry (open squares) and wet season (black circles). The dashed line is the function proposed by Moran et al., 1994: $\alpha = 0.583 \exp(-2.13\ NDVI)$, the cross-line is the formula of Bastiaanssen et al. (2000) $\alpha = 0.20\ (1-0.96\ NDVI^4)$. The continuous curve is the function proposed by Su (2002): $\alpha = \alpha_0 + (\alpha_{max}-\alpha_0)\ (1-f_c)$ where $\alpha_0 = 0.05$ and $\alpha_{max}=0.315$. f_c being the cover vegetation fraction computed as $f_c = (NDVI-NDVI_{min})^2/(NDVI_{max}-NDVI_{min})^2$, with $NDVI_{min} = 0.08$ (observed at Eguerit) and $NDVI_{max} = 0.86$ (observed at Bellefoungou).*

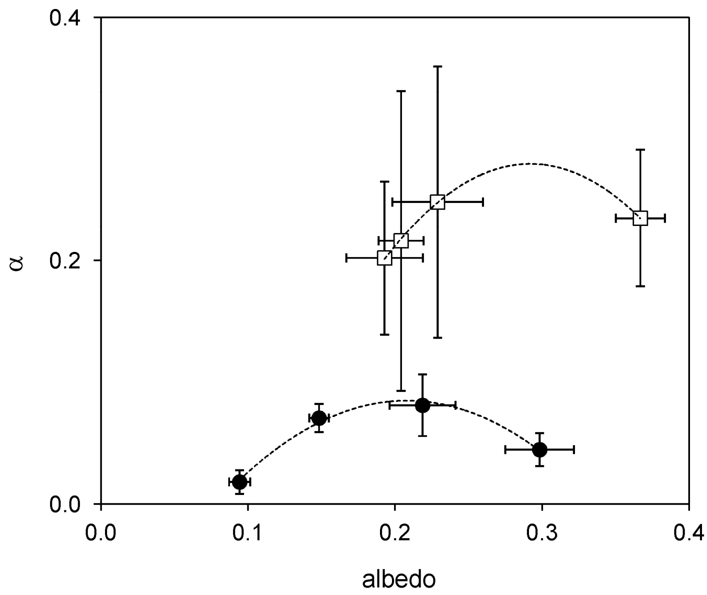

Figure 5: *Evolution of α vs albedo for the dry (open squares) and wet (black circles) season.*

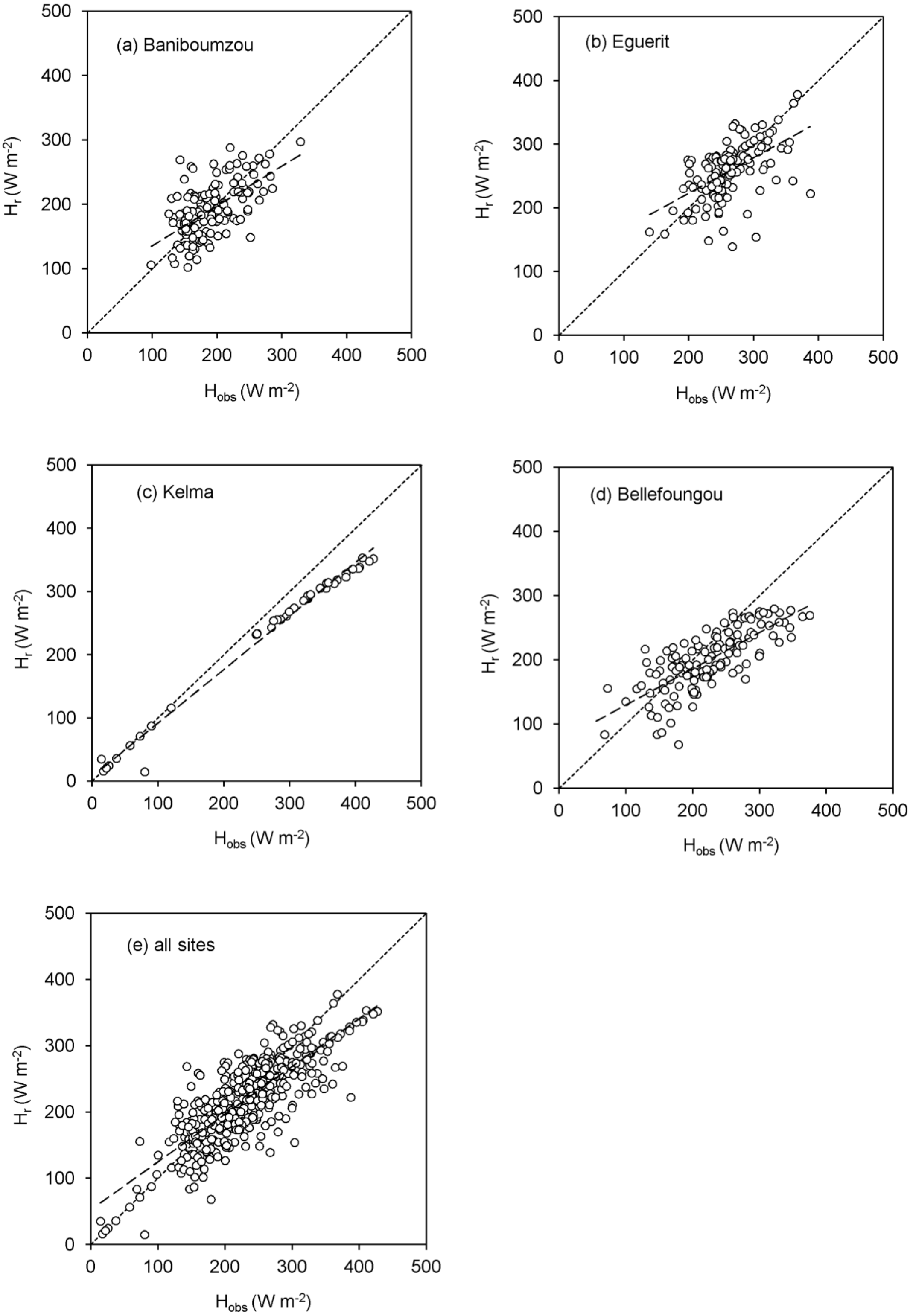

Figure 6. *Comparison between retrieved (using Par-1) and observed sensible heat flux for (a) Banizoumbou (b) Eguerit (c) Kelma (d) Bellefoungo (e) all sites (pooled data). Dashed lines = linear regression, dotted lines = 1:1 relationship.*

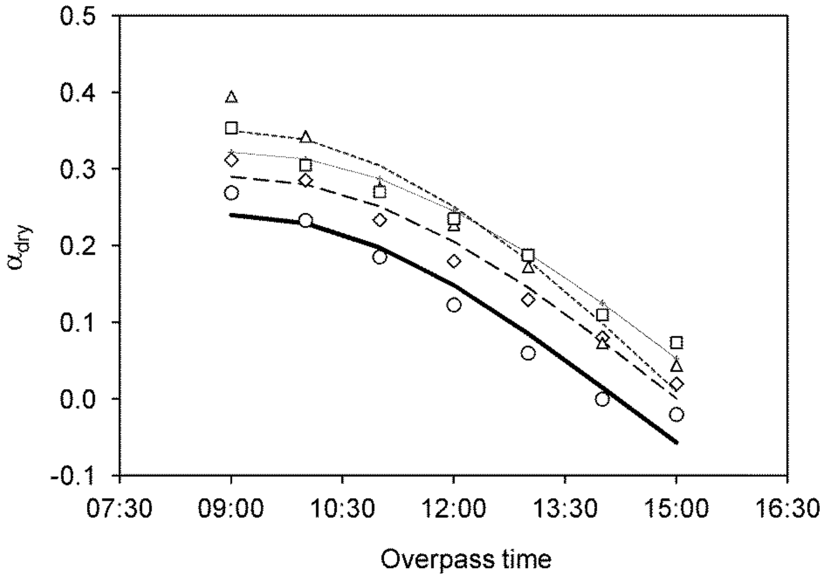

Figure 7: *Values of α_{dry} for each hour of the period 9.00 to 15.00 h. Symbols: circles = Bellefoungou; squares = Kelma; triangles = Eguerit; diamond =Banizoumbou. The curves are the best fit of Eq. 12 (SF-model) to the points.*

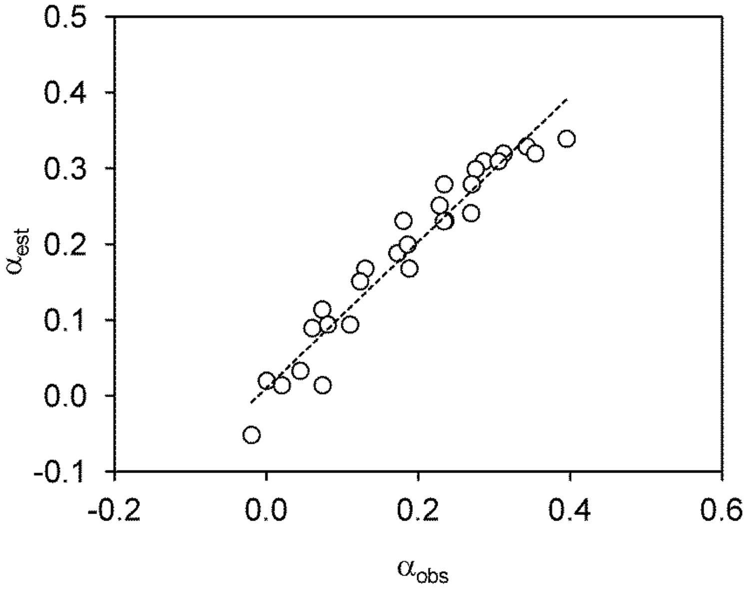

Figure 8: *Relationship between observed (α_{obs}) and estimated (α_{est}) values of $\alpha = G/R_n$. Estimates from the SF-model with A_{dry} and B_{dry} given by Eqs. 13 and 14. The line is the linear regression α_{est}.= 0.96 α_{obs} + 0.01 (R^2= 0.94, RMSE = 0.029)*